Lecture 16: Particle Image Velocimetry (PIV) - Part 03

Dr. Hui Hu

Martin C. Jischke Professor in Aerospace Engineering
Dept. of Aerospace Engineering, Iowa State University
537 Bissell Road, Ames, Iowa 50011-1096, USA.
Tel: 515-294-0094 (O) / Fax: 515-294-3262 (O)
Email: huhui@iastate.edu

❑ Comparison between PIV and PTV

- *Particle Tracking Velocimetry:*
  - *Tracking individual particle*
  - *Limited to low particle image density case*
  - *Velocity vector at random points where tracer particles exist.*
  - *Spatial resolution of PTV results is usually limited by the number of the tracer particles*

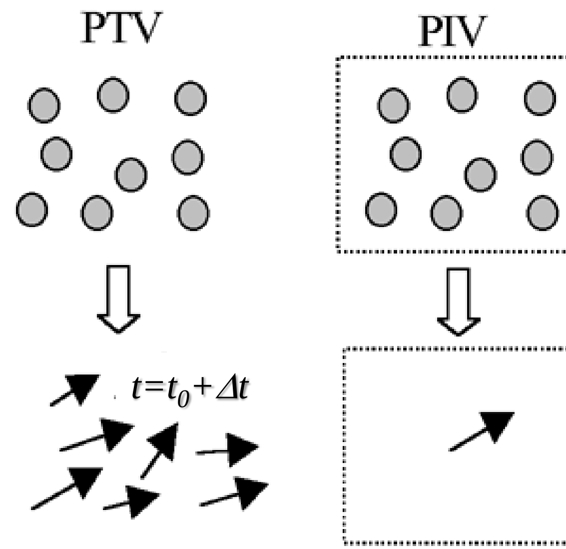

- *Correlation-based PIV:*
  - *Tracking a group of particles*
  - *Applicable to high particle image density case*
  - *Spatial resolution of PIV results is usually limited by the size of the interrogation window size*
  - *Velocity vector can be at regular grid points.*

PTV

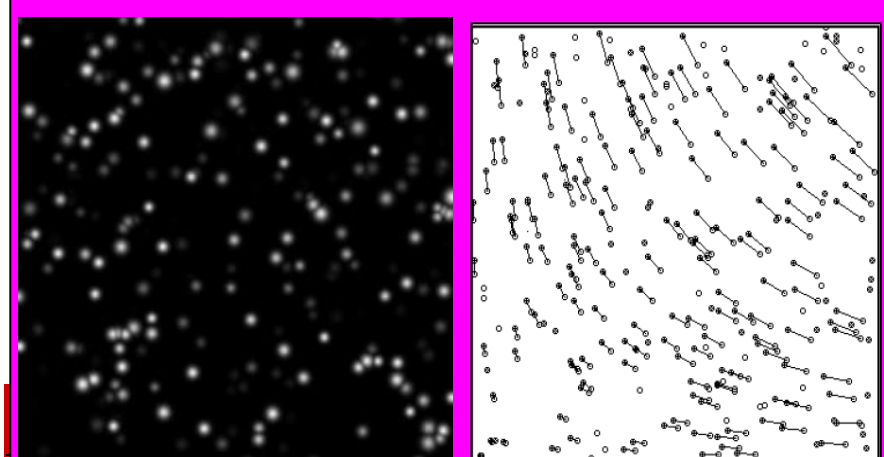

PIV

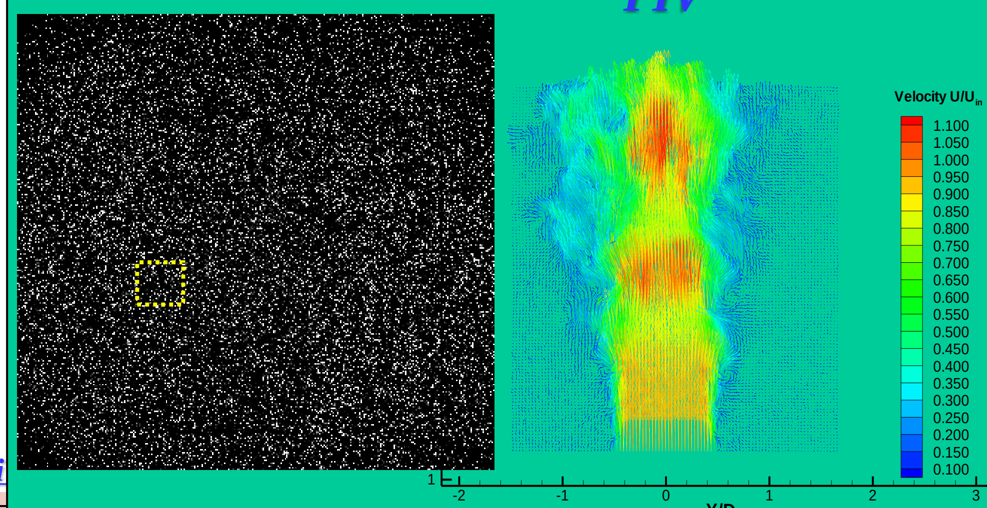

❑ Multiple-correlation validation technique

- *Since the noise peak in the correlation space may be randomly, causing the multiplied value to be reduced to zero. Thus, the correct peak can be easily identified.*
- *The location of the correct peak in the correlation space is corresponding to the averaged movement of the overlap region*

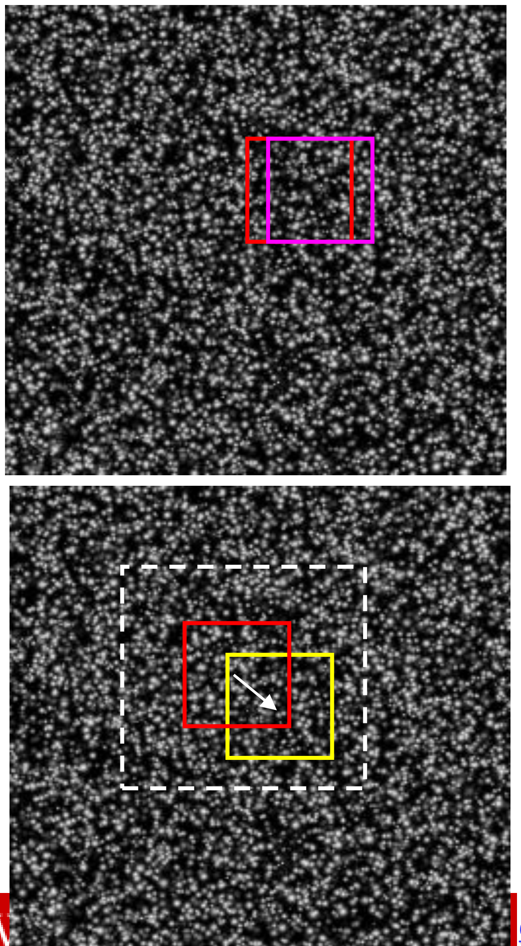

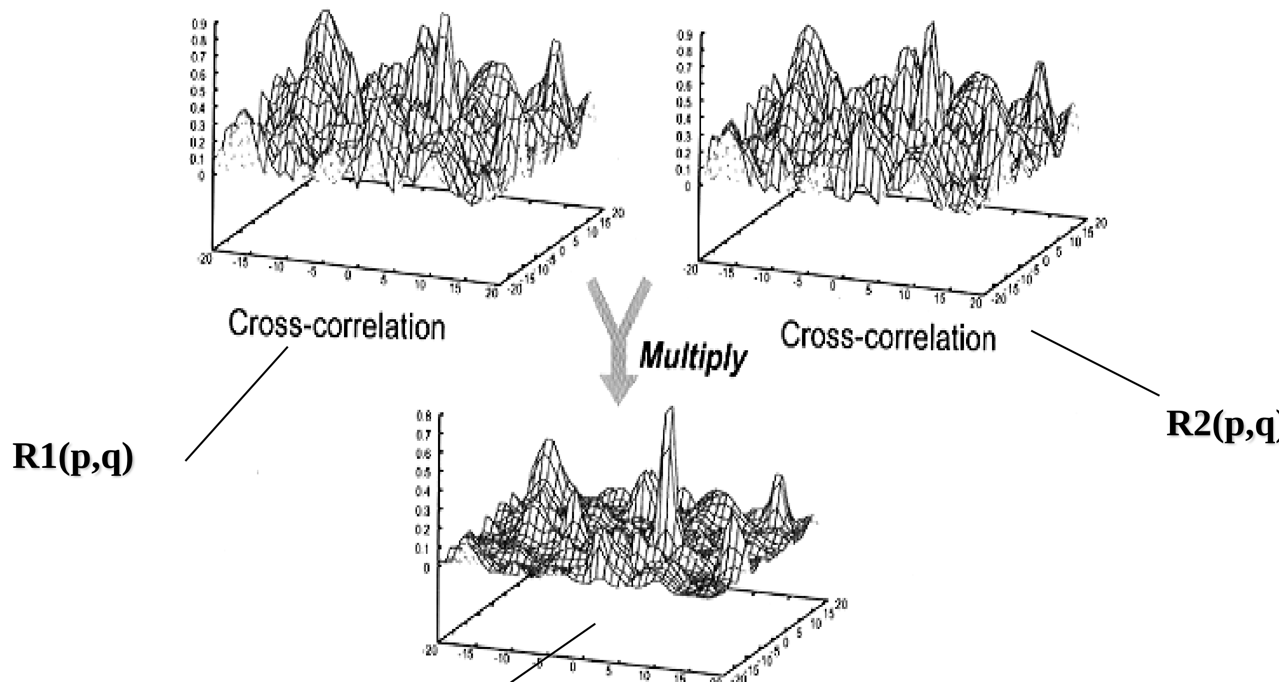

$$R_{(p,q)} = R_{1(p,q)} * R_{2(p,q)}$$

❑ The comparison of various PIV methods

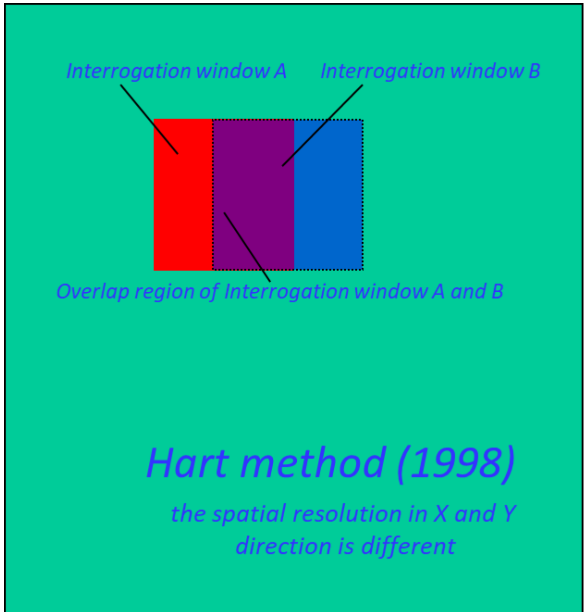

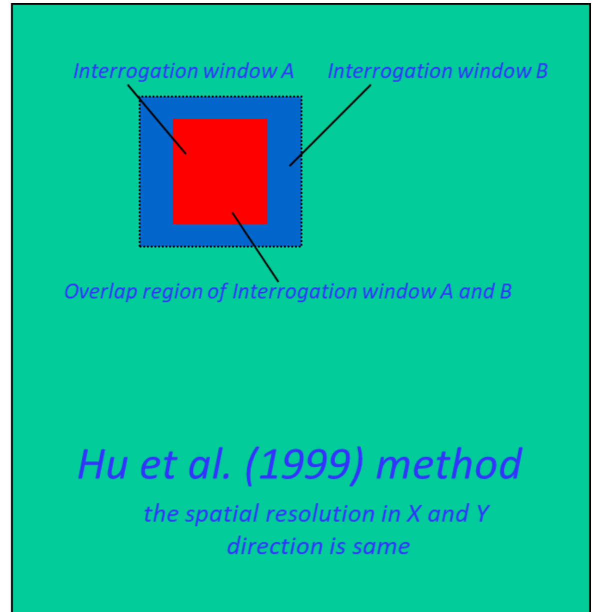

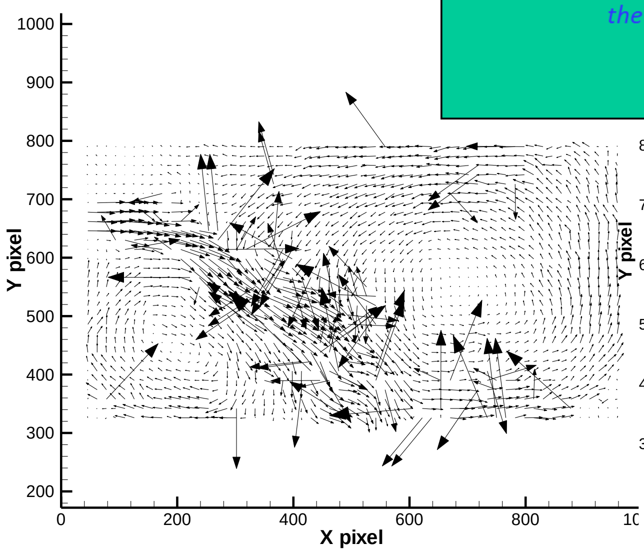

a. FFT-CC method
(interrogation window: 32 by 32 pixel)

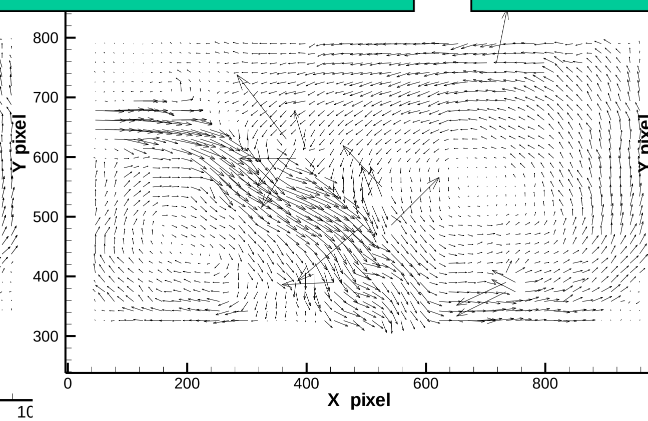

b. D-CC method
(interrogation window: 32 by 32 pixel)

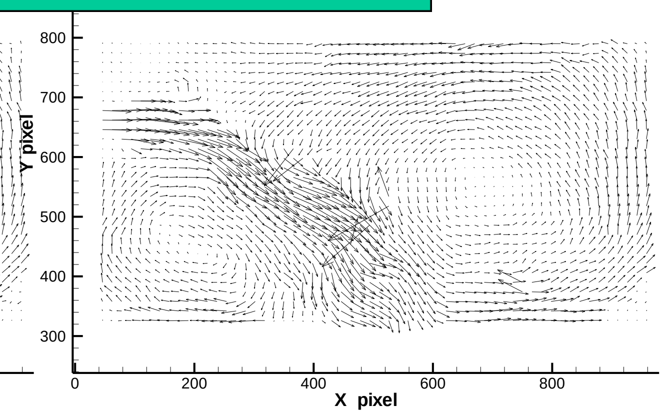

c. D-CC methodwith correlation error correction treatment
(interrogation window: 32 by 32 pixel)

❑ The Effect of the Size of the Interrogation Window

Real flow field

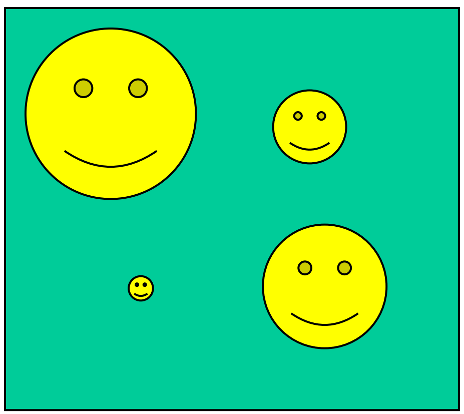

Image processing

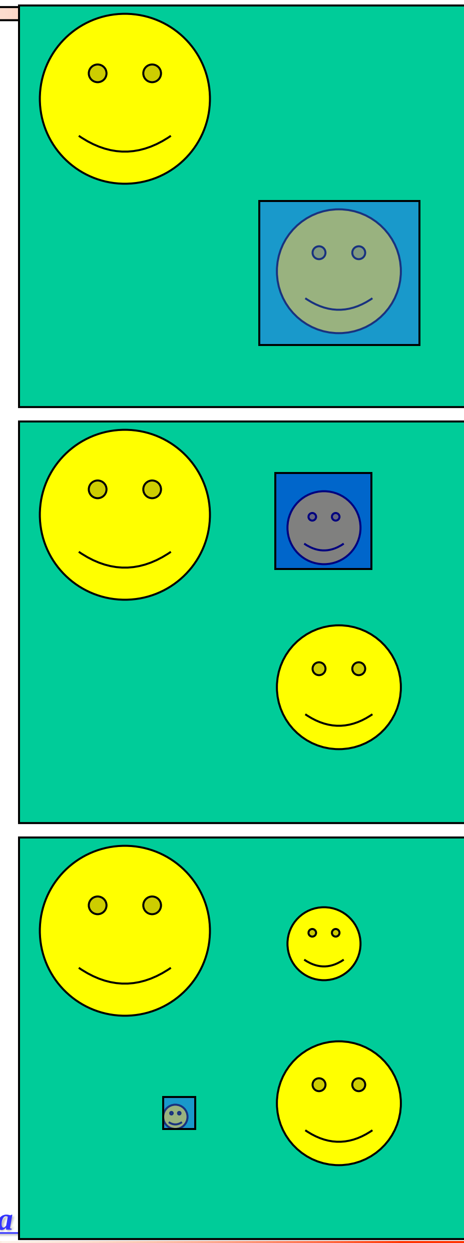

PIV final result

Vortical structure

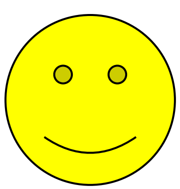

Interrogation window

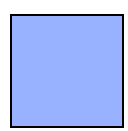

❑ Hierarchical Recursive PIV Algorithm

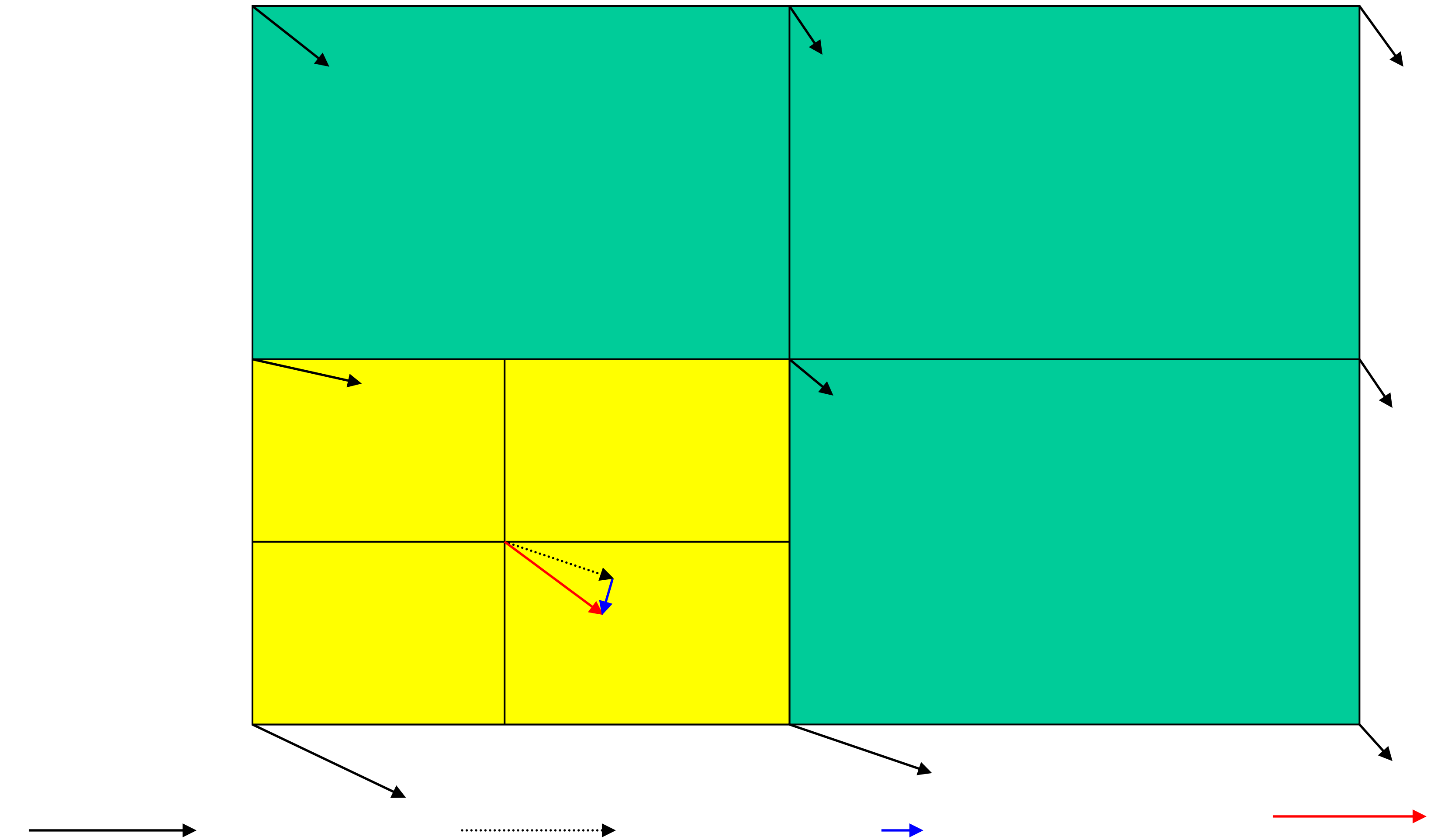

❑ Results from Hierarchical PIV algorithm

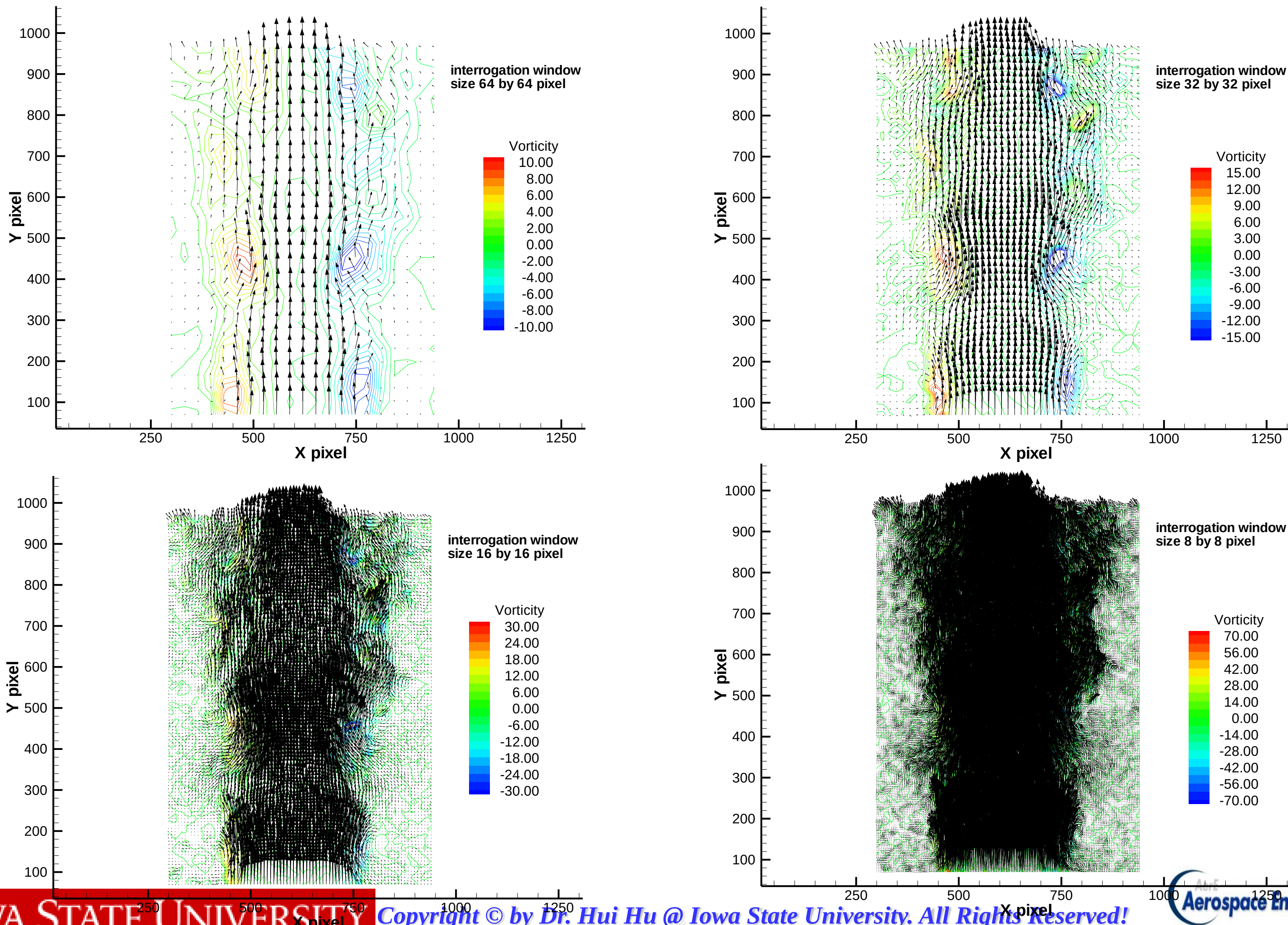

❑ Results with different interrogation window size

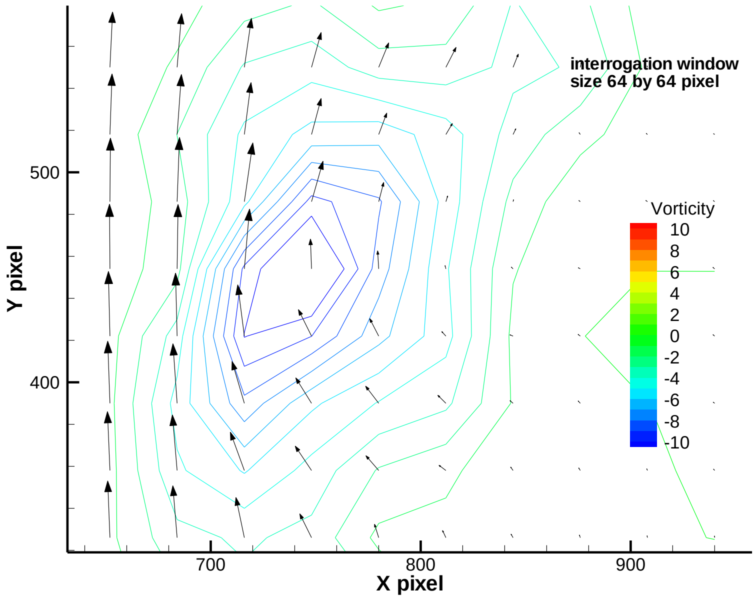

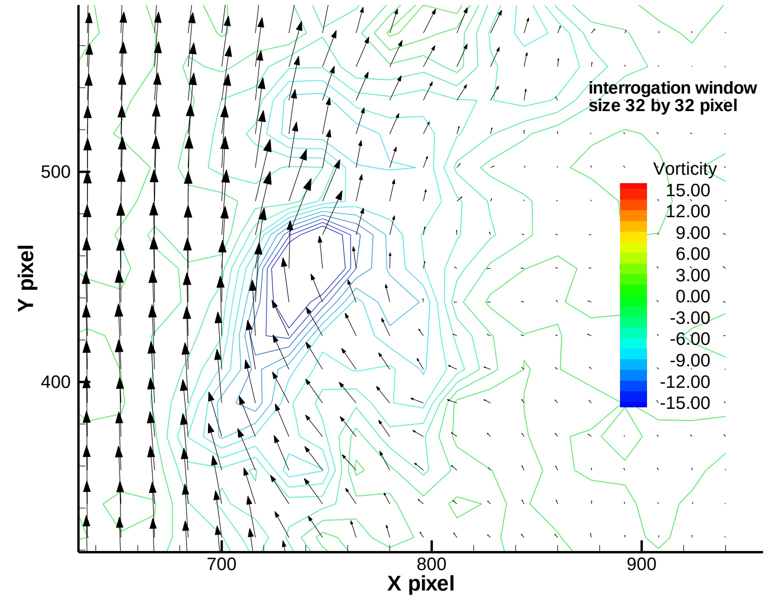

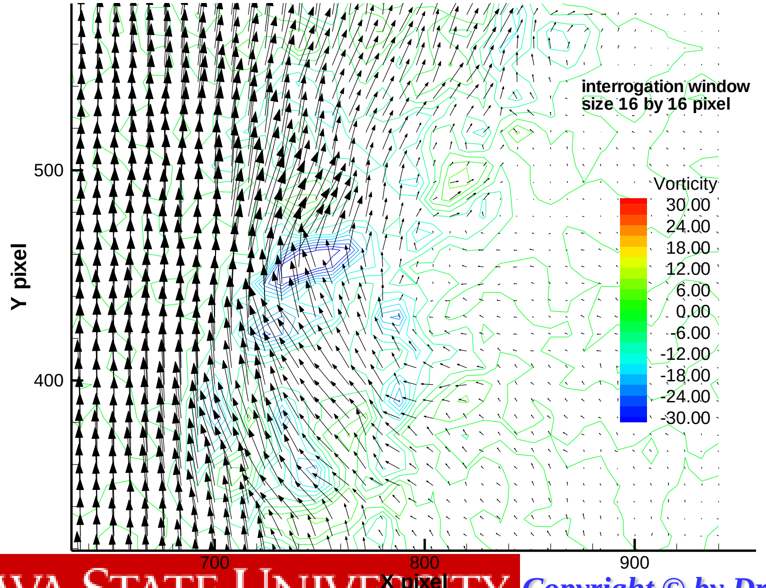

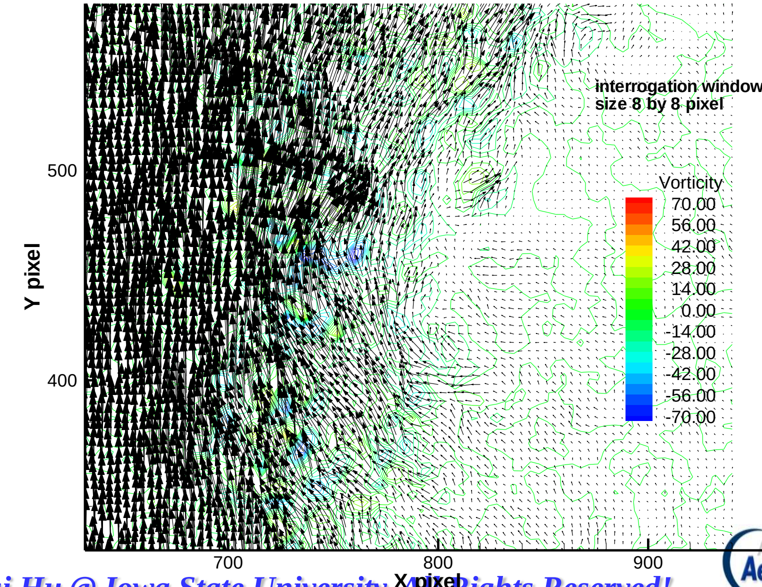

❑ The effect of the spatial resolution of PIV result

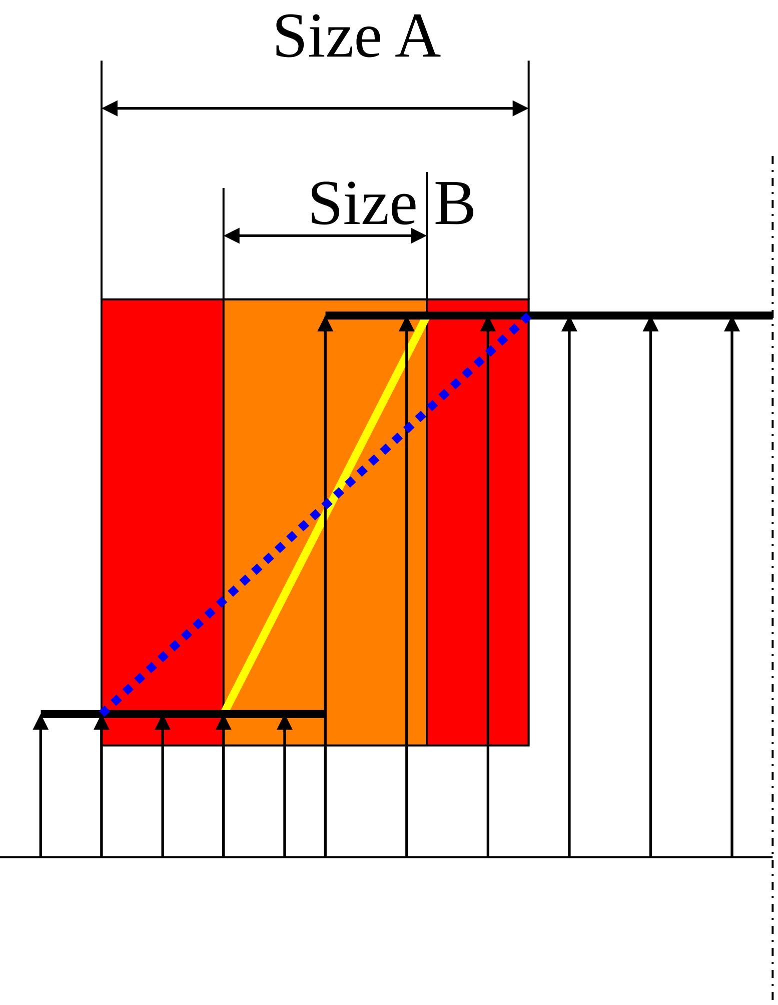

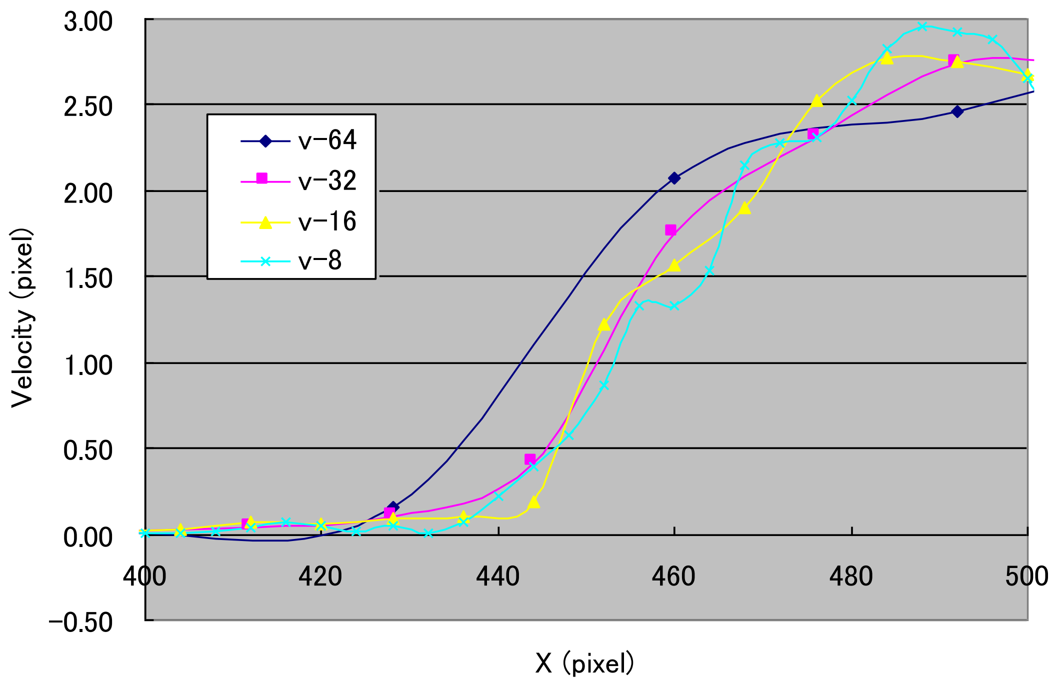

❑ Application on the Lobed Jet Flow Research

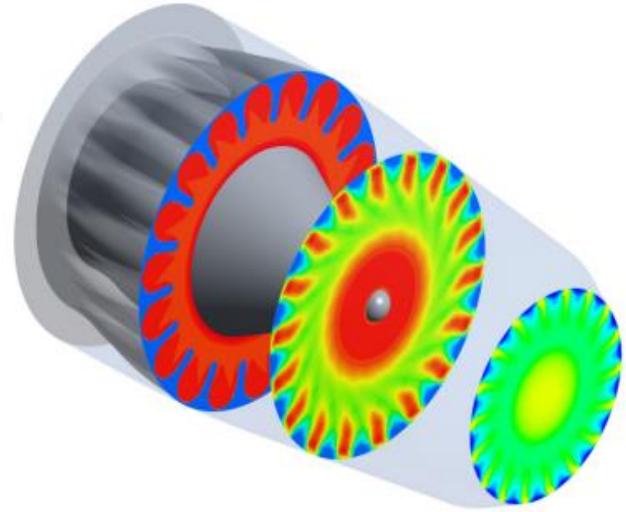

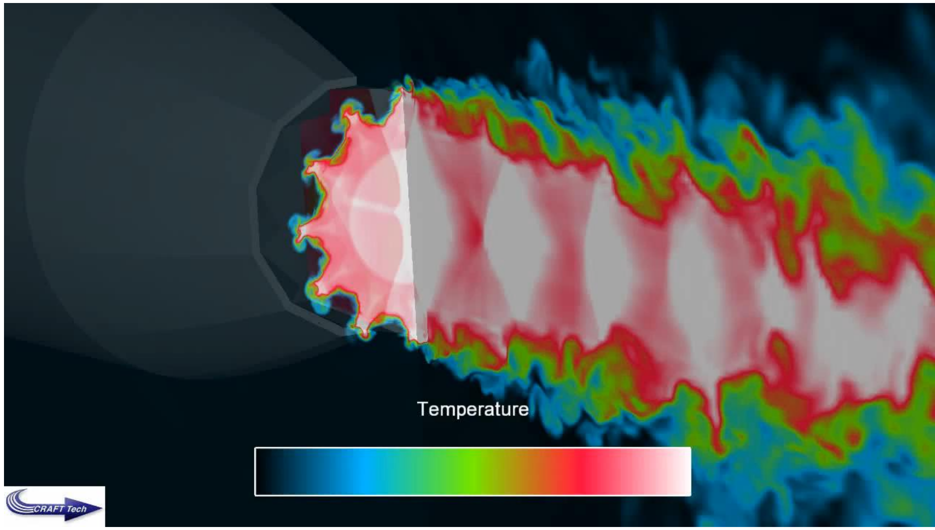

❑ APPLICATION ON LOBED JET FLOW

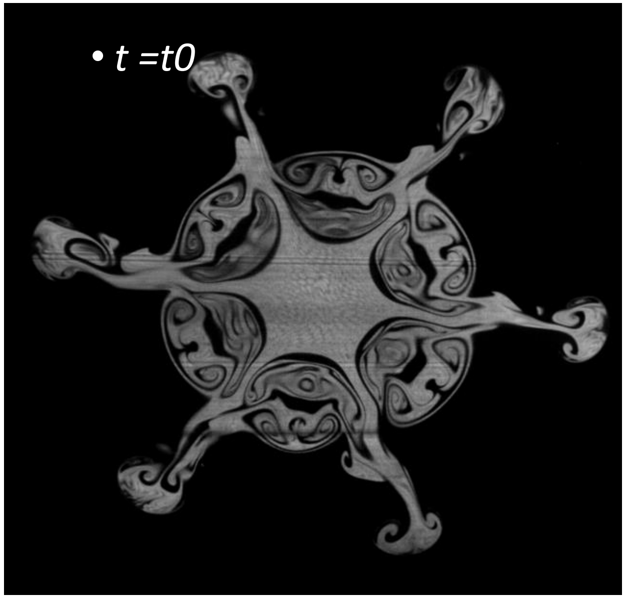

A. interrogation window size - 64 by 64 pixel

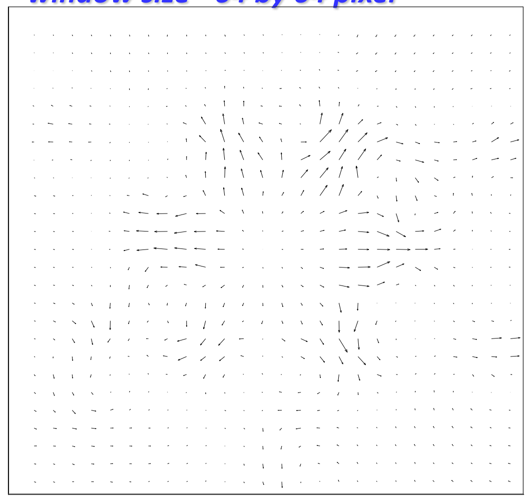

B. interrogation window size - 32 by 32 pixel

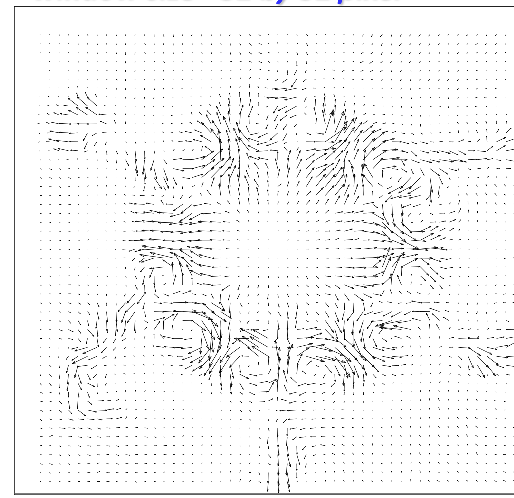

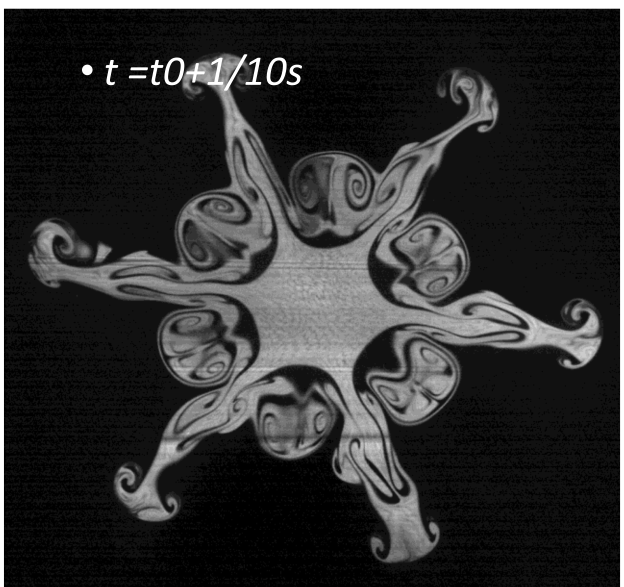

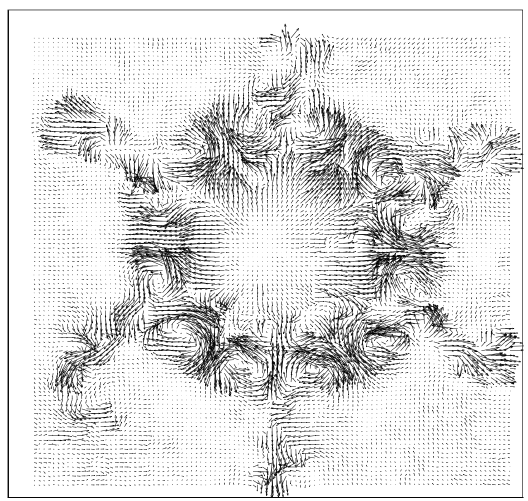

C. interrogation window size - 16 by 16 pixel

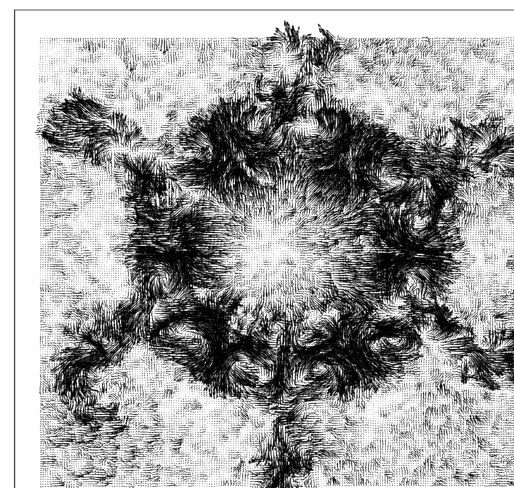

D. interrogation window size 8 by 8 pixel

❑ Velocity power spectrum with different spatial resolution levels

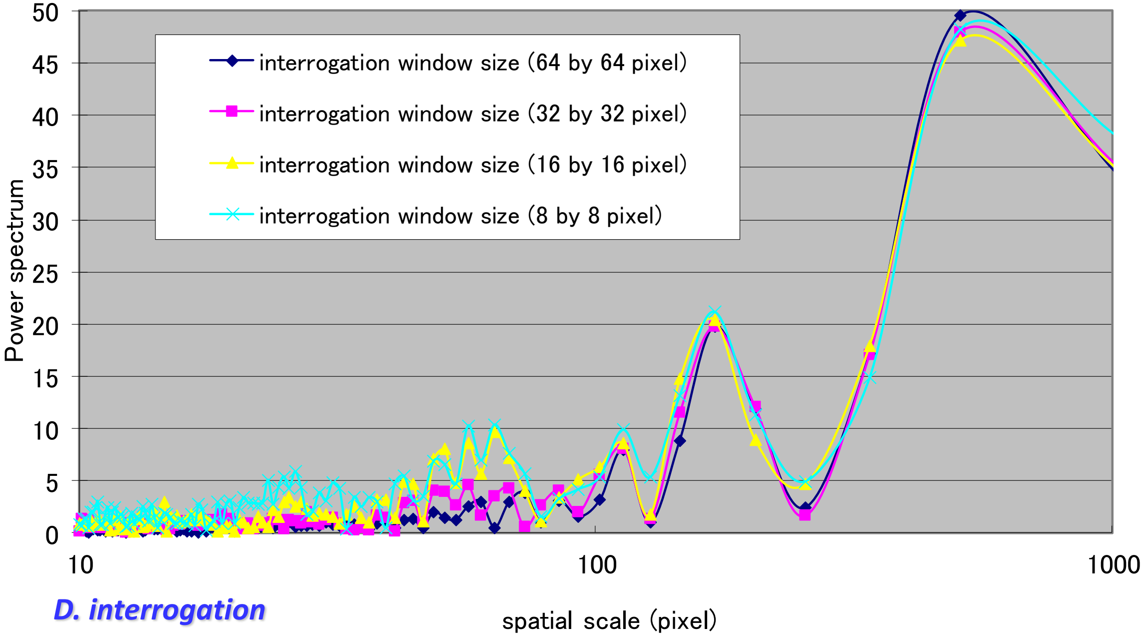

B. interrogation window size - 32 by 32 pixel

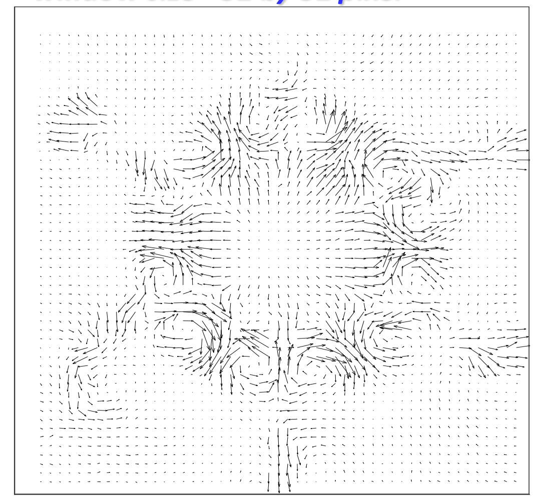

D. interrogation window size 8 by 8 pixel

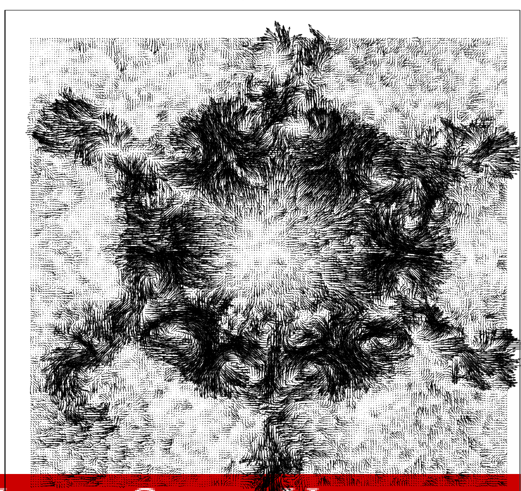

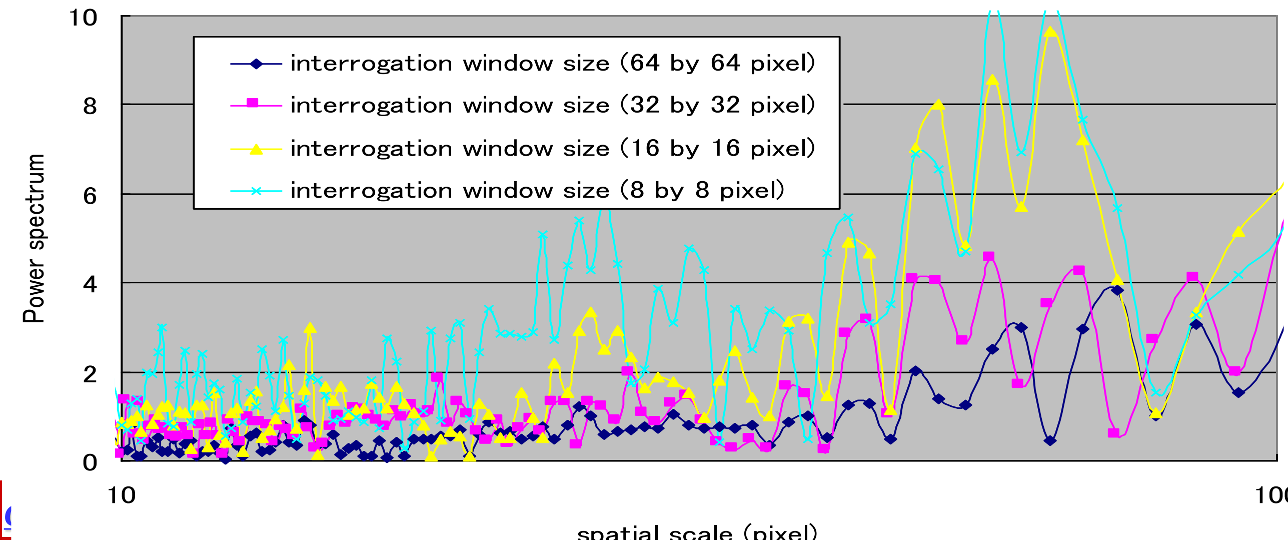

❑ Post processing of PIV measurements

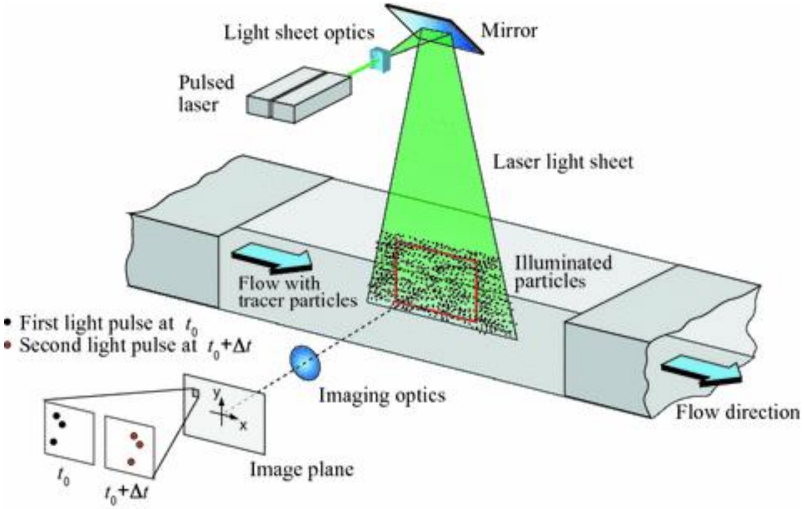

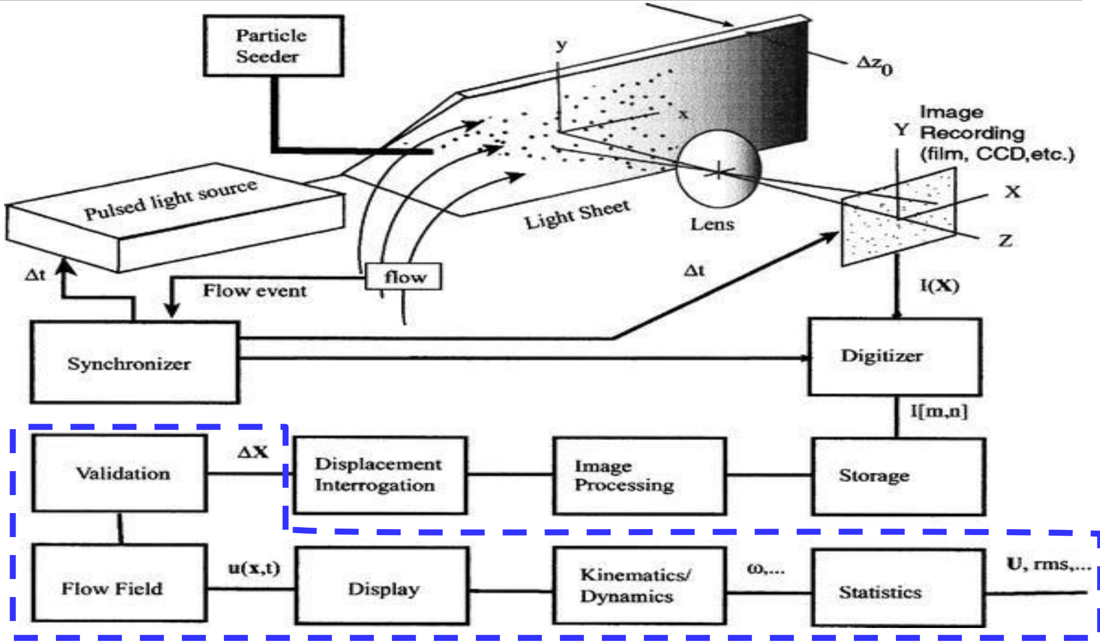

a. T=t0

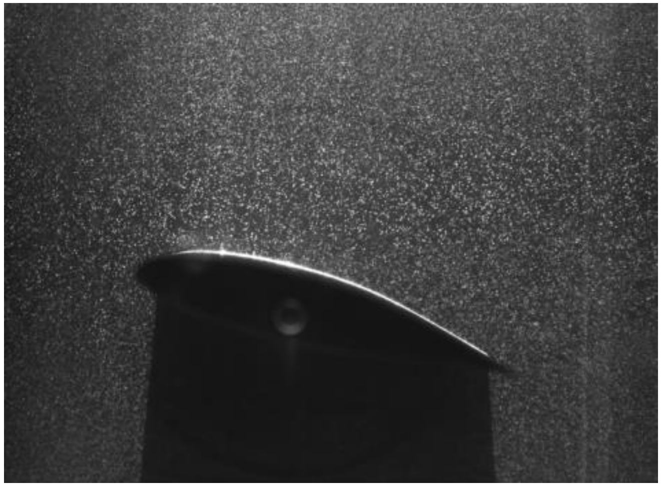

b. T=t0+10μs

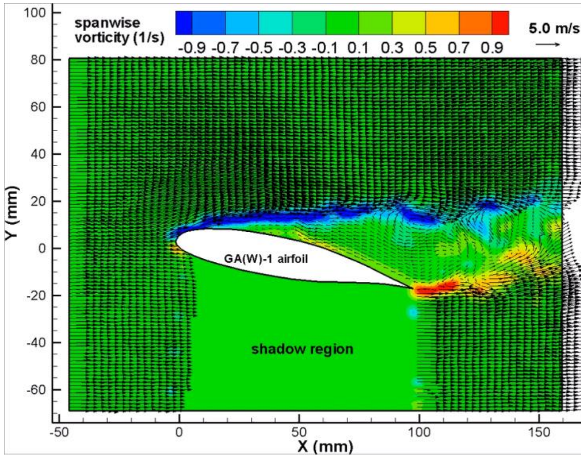

Corresponding Velocity field

❑ PIV Results

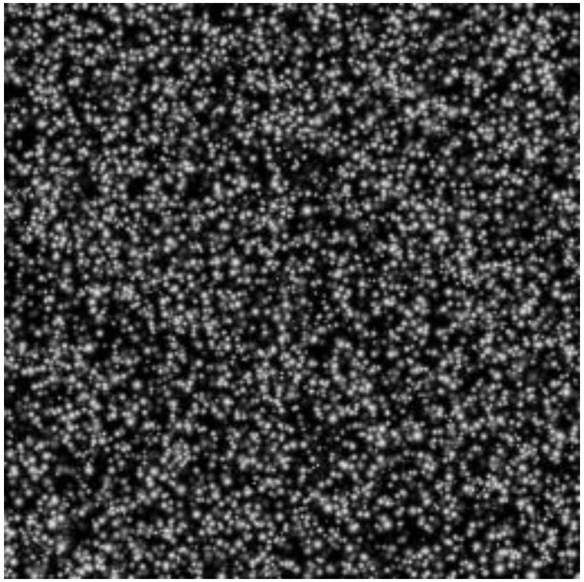

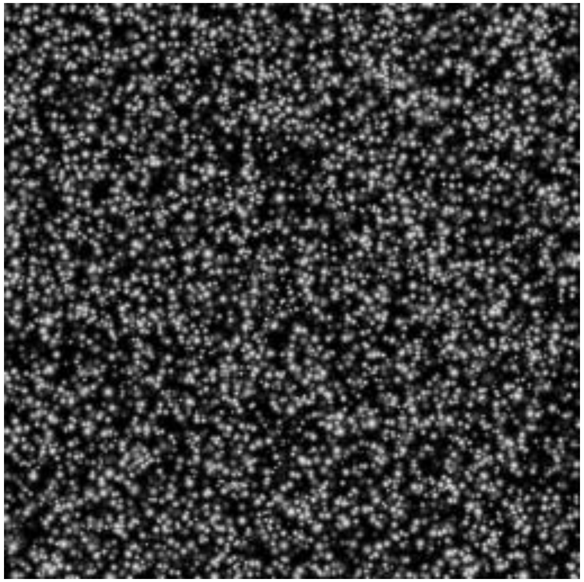

a. $t=t_0$

b. $t=t_0+\Delta t$

PIV image pair

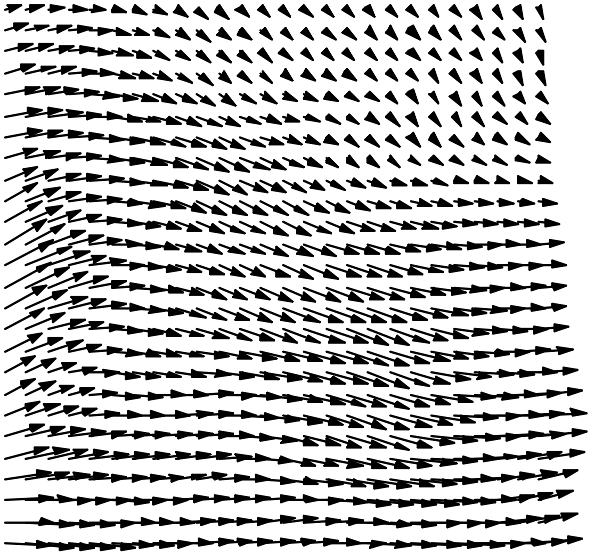

Corresponding flow velocity field

❑ Post processing: Detection of spurious vectors

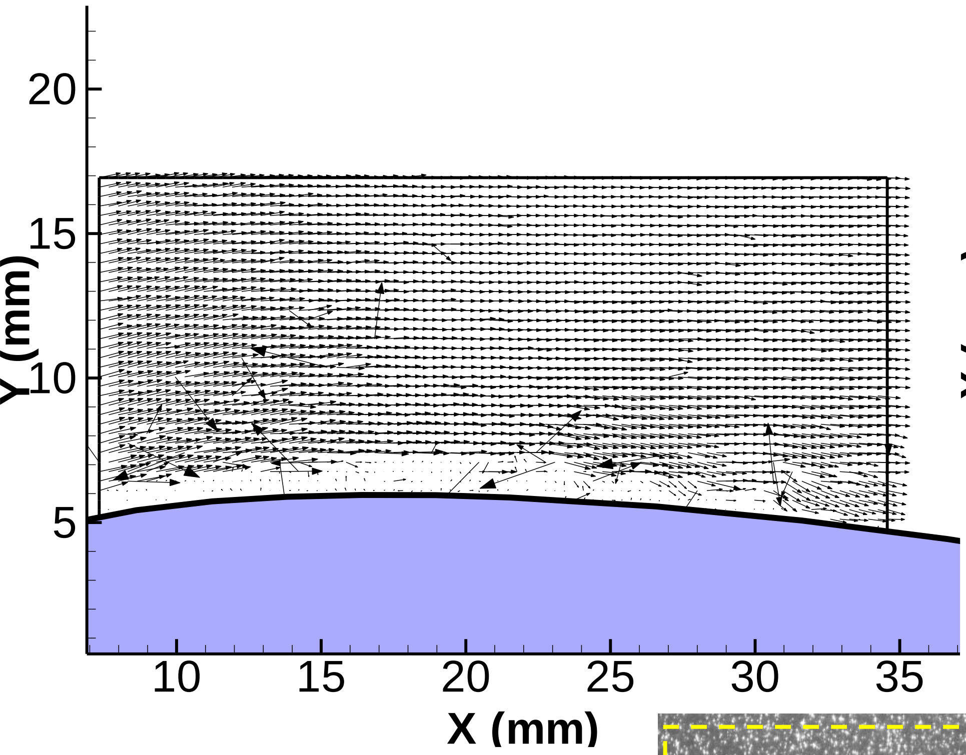

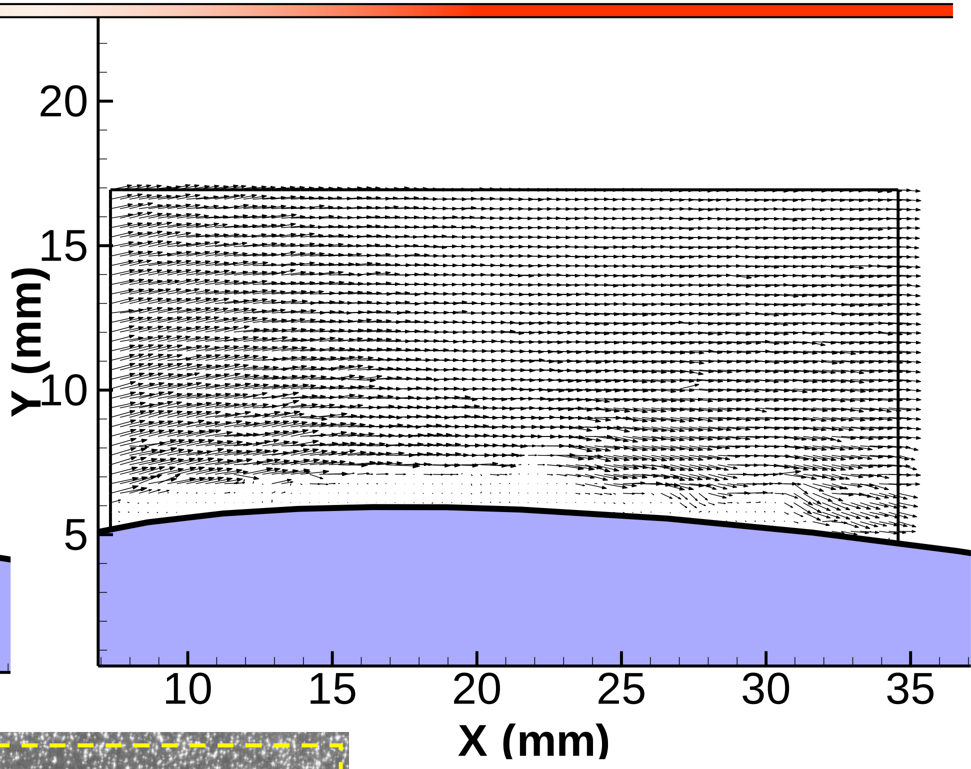

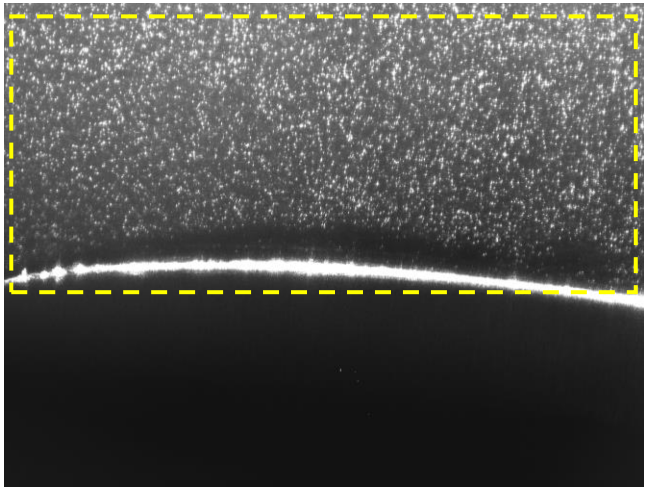

Detection of spurious vectors

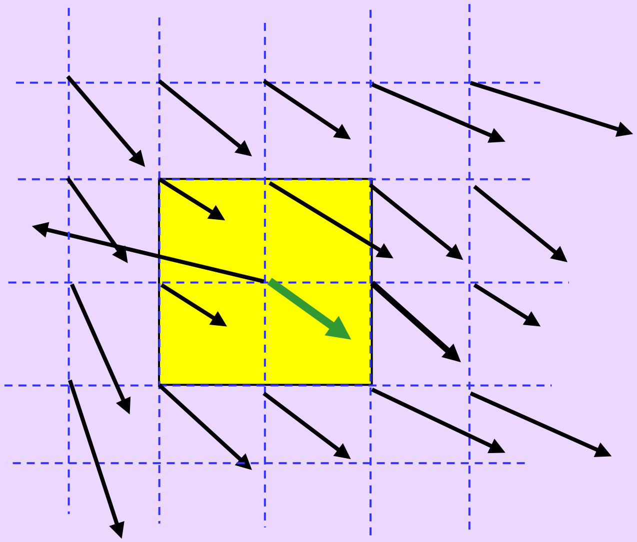

$$Um = \frac{U_{i+1,j-1} + U_{i+1,j} + U_{i+1,j+1} + U_{i,j-1} + U_{i,j+1} + U_{i-1,j-1} + U_{i-1,j} + U_{i-1,j+1}}{8}$$

$$Vm = \frac{V_{i+1,j-1} + V_{i+1,j} + V_{i+1,j+1} + V_{i,j-1} + V_{i,j+1} + V_{i-1,j-1} + V_{i-1,j} + V_{i-1,j+1}}{8}$$

$$R\_value = \frac{\sqrt{(U_{i,j} - Um)^2 + (V_{i,j} - Vm)^2}}{\sqrt{Um^2 + Vm^2}} \approx \frac{\sqrt{(U_{i,j} - Um)^2 + (V_{i,j} - Vm)^2}}{\sqrt{Um^2 + Vm^2} + \varepsilon}$$

ε: is a very small number, such as 0.000000001.

$R\_value > R_{thresh\_hold}$ for a spurious vector

Regular method

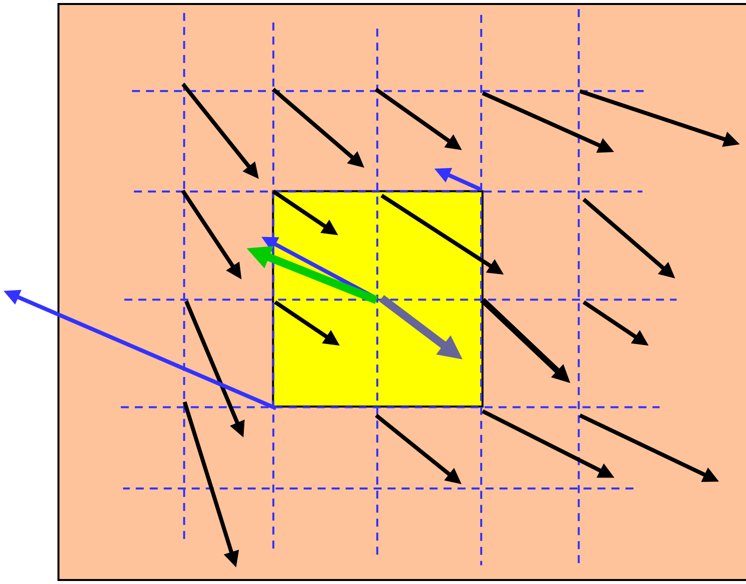

$$Um = \frac{U_{i+1,j-1} + U_{i+1,j} + U_{i+1,j+1} + U_{i,j-1} + U_{i,j+1} + U_{i-1,j-1} + U_{i-1,j} + U_{i-1,j+1} - U\max - U\min}{6}$$

$$Vm = \frac{V_{i+1,j-1} + V_{i+1,j} + V_{i+1,j+1} + V_{i,j-1} + V_{i,j+1} + V_{i-1,j-1} + V_{i-1,j} + V_{i-1,j+1} - V\max - V\min}{6}$$

$$R\_value = \frac{\sqrt{(U_{i,j} - Um)^2 + (V_{i,j} - Vm)^2}}{\sqrt{Um^2 + Vm^2}} \approx \frac{\sqrt{(U_{i,j} - Um)^2 + (V_{i,j} - Vm)^2}}{\sqrt{Um^2 + Vm^2} + \varepsilon}$$

ε: is a very small number, such as 0.000000001.

$R\_value > R_{thresh\_hold}$ for a spurious vector

Median test method

❑ Estimation of differential quantities

$$\frac{\mathrm{d}\boldsymbol{U}}{\mathrm{d}\boldsymbol{X}} = \begin{bmatrix} \frac{\partial U}{\partial X} & \frac{\partial V}{\partial X} & \frac{\partial W}{\partial X} \\ \frac{\partial U}{\partial Y} & \frac{\partial V}{\partial Y} & \frac{\partial W}{\partial Y} \\ \frac{\partial U}{\partial Z} & \frac{\partial V}{\partial Z} & \frac{\partial W}{\partial Z} \end{bmatrix} \tag{6.7}$$

This deformation tensor can be decomposed into a symmetric part and an antisymmetric part:

$$\frac{\mathrm{d}\boldsymbol{U}}{\mathrm{d}\boldsymbol{X}} = \begin{bmatrix} \frac{\partial U}{\partial X} & \frac{1}{2}\left(\frac{\partial V}{\partial X}+\frac{\partial U}{\partial Y}\right) & \frac{1}{2}\left(\frac{\partial W}{\partial X}+\frac{\partial U}{\partial Z}\right) \\ \frac{1}{2}\left(\frac{\partial U}{\partial Y}+\frac{\partial V}{\partial X}\right) & \frac{\partial V}{\partial Y} & \frac{1}{2}\left(\frac{\partial W}{\partial Y}+\frac{\partial V}{\partial Z}\right) \\ \frac{1}{2}\left(\frac{\partial U}{\partial Z}+\frac{\partial W}{\partial X}\right) & \frac{1}{2}\left(\frac{\partial V}{\partial Z}+\frac{\partial W}{\partial Y}\right) & \frac{\partial W}{\partial Z} \end{bmatrix} \tag{6.8}$$

$$+ \begin{bmatrix} 0 & \frac{1}{2}\left(\frac{\partial V}{\partial X}-\frac{\partial U}{\partial Y}\right) & \frac{1}{2}\left(\frac{\partial W}{\partial X}-\frac{\partial U}{\partial Z}\right) \\ \frac{1}{2}\left(\frac{\partial U}{\partial Y}-\frac{\partial V}{\partial X}\right) & 0 & \frac{1}{2}\left(\frac{\partial W}{\partial Y}-\frac{\partial V}{\partial Z}\right) \\ \frac{1}{2}\left(\frac{\partial U}{\partial Z}-\frac{\partial W}{\partial X}\right) & \frac{1}{2}\left(\frac{\partial V}{\partial Z}-\frac{\partial W}{\partial Y}\right) & 0 \end{bmatrix} \tag{6.9}$$

A substitution of the strain and vorticity components yields:

$$\frac{\mathrm{d}\boldsymbol{U}}{\mathrm{d}\boldsymbol{X}} = \begin{bmatrix} \epsilon_{XX} & \frac{1}{2}\epsilon_{XY} & \frac{1}{2}\epsilon_{XZ} \\ \frac{1}{2}\epsilon_{YX} & \epsilon_{YY} & \frac{1}{2}\epsilon_{YZ} \\ \frac{1}{2}\epsilon_{ZX} & \frac{1}{2}\epsilon_{ZY} & \epsilon_{ZZ} \end{bmatrix} + \begin{bmatrix} 0 & \frac{1}{2}\omega_Z & -\frac{1}{2}\omega_X \\ -\frac{1}{2}\omega_Z & 0 & \frac{1}{2}\omega_Y \\ -\frac{1}{2}\omega_X & \frac{1}{2}\omega_Y & 0 \end{bmatrix} \tag{6.10}$$

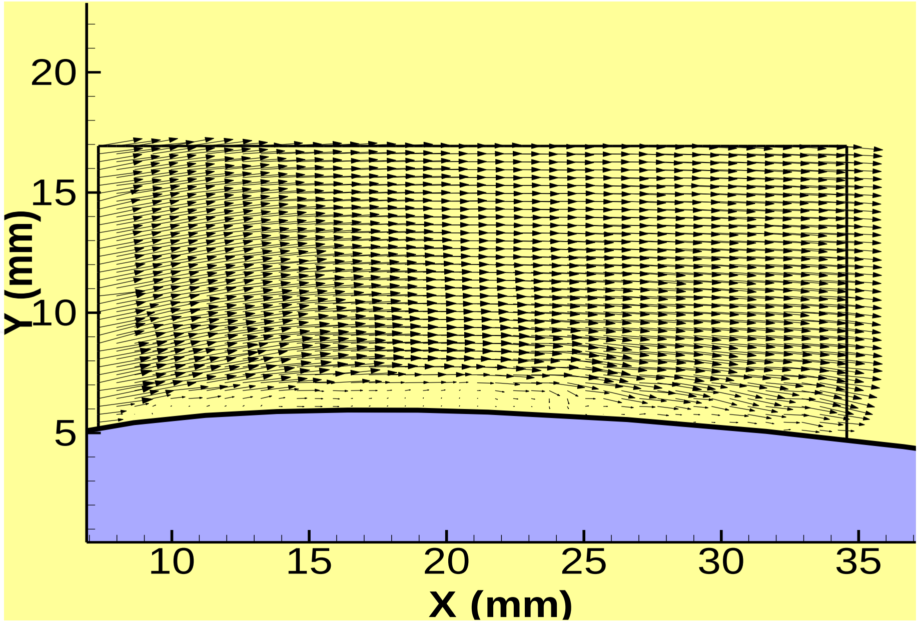

Operator	Implementation	Accuracy	Uncertainty
Forward difference	$\left(\frac{\mathrm{d}f}{\mathrm{d}x}\right)_{i+1/2} \approx \frac{f_{i+1}-f_i}{\Delta X}$	$O(\Delta X)$	$\approx 1.41\frac{\epsilon_U}{\Delta X}$
Backward difference	$\left(\frac{\mathrm{d}f}{\mathrm{d}x}\right)_{i-1/2} \approx \frac{f_i-f_{i-1}}{\Delta X}$	$O(\Delta X)$	$\approx 1.41\frac{\epsilon_U}{\Delta X}$
Center difference	$\left(\frac{\mathrm{d}f}{\mathrm{d}x}\right)_i \approx \frac{f_{i+1}-f_{i-1}}{2\Delta X}$	$O(\Delta X^2)$	$\approx 0.7\frac{\epsilon_U}{\Delta X}$
Richardson extrapol.	$\left(\frac{\mathrm{d}f}{\mathrm{d}x}\right)_i \approx \frac{f_{i-2}-8f_{i-1}+8f_{i+1}-f_{i+2}}{12\Delta X}$	$O(\Delta X^3)$	$\approx 0.95\frac{\epsilon_U}{\Delta X}$
Least squares	$\left(\frac{\mathrm{d}f}{\mathrm{d}x}\right)_i \approx \frac{2f_{i+2}+f_{i+1}-f_{i-1}-2f_{i-2}}{10\Delta X}$	$O(\Delta X^2)$	$\approx 1.0\frac{\epsilon_U}{\Delta X}$

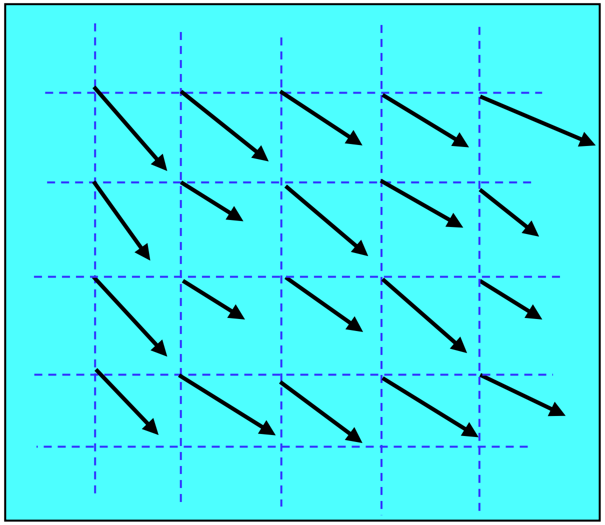

❑ Estimation of Vorticity distribution

$$\varpi_z = \frac{\partial V}{\partial x} - \frac{\partial U}{\partial y}$$

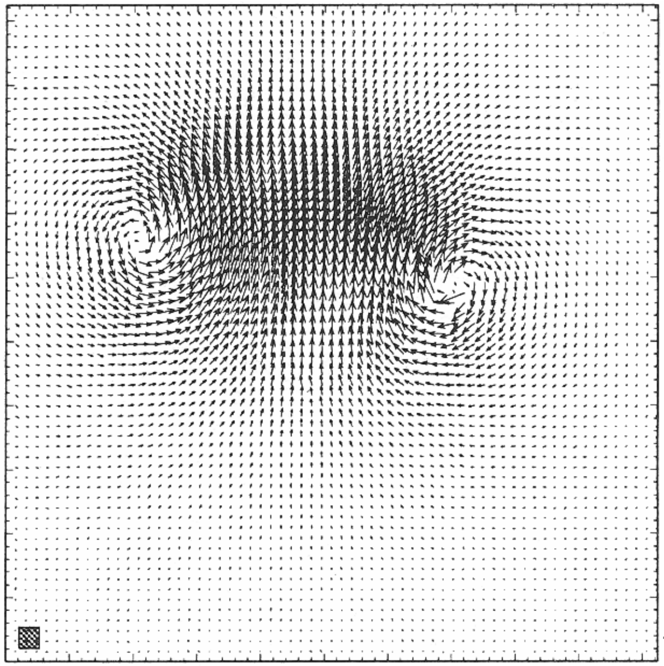

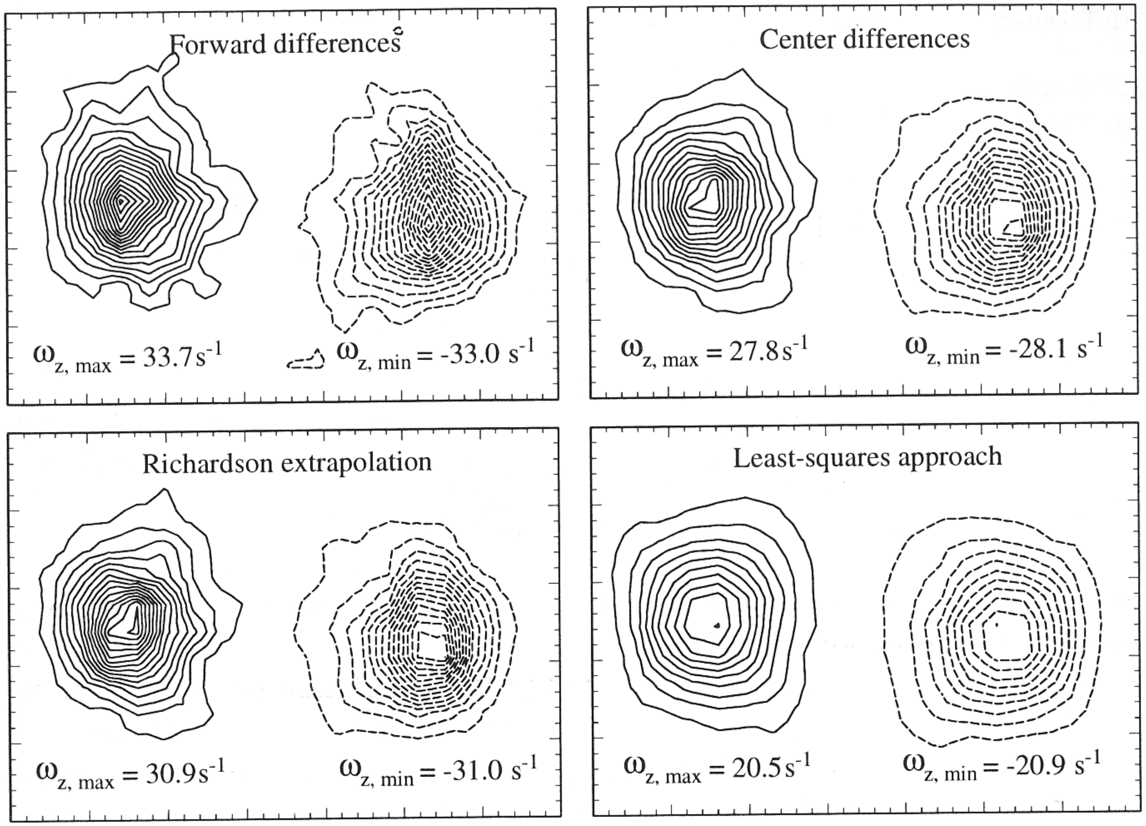

Fig. 6.7. Vorticity field estimates obtained from twice oversampled PIV data, e.g. the interrogation window overlap is 50%. The vortex pair is known to be laminar and thus should have smooth vorticity contours

❑ Estimation of Vorticity distribution

Stokes Theorem:

$$\Gamma = -\oint_C \vec{V}\, d\vec{l} = -\iint_S \vec{\varpi} \bullet d\vec{A}$$

$$\Rightarrow \varpi_z = \frac{\Gamma_{x-y}}{dA}$$

$$(\omega_Z)_{i,j} \;\widehat{=}\; \frac{\Gamma_{i,j}}{4\Delta X \Delta Y}$$

with

$$\begin{aligned}\Gamma_{i,j} &= \frac{1}{2}\Delta X\left(U_{i-1,j-1} + 2U_{i,j-1} + U_{i+1,j-1}\right)\\ &+ \frac{1}{2}\Delta Y\left(V_{i+1,j-1} + 2V_{i+1,j} + V_{i+1,j+1}\right)\\ &- \frac{1}{2}\Delta X\left(U_{i+1,j+1} + 2U_{i,j+1} + U_{i-1,j+1}\right)\\ &- \frac{1}{2}\Delta Y\left(V_{i-1,j+1} + 2V_{i-1,j} + V_{i-1,j-1}\right)\end{aligned}$$

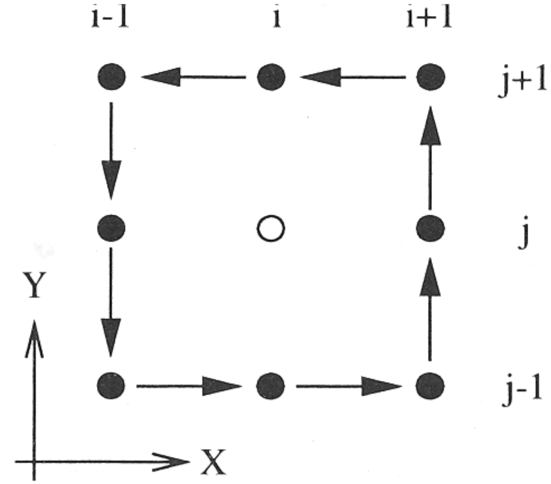

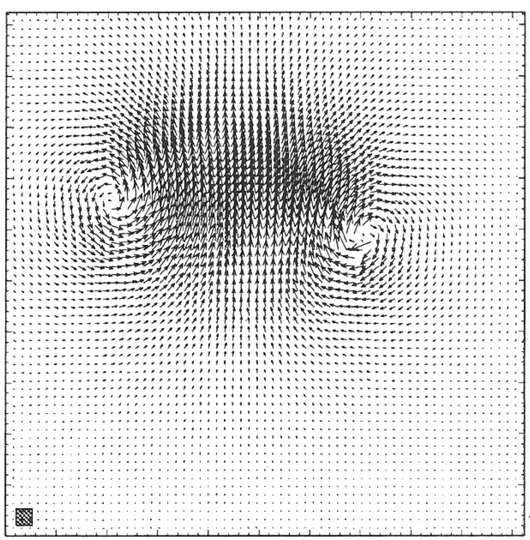

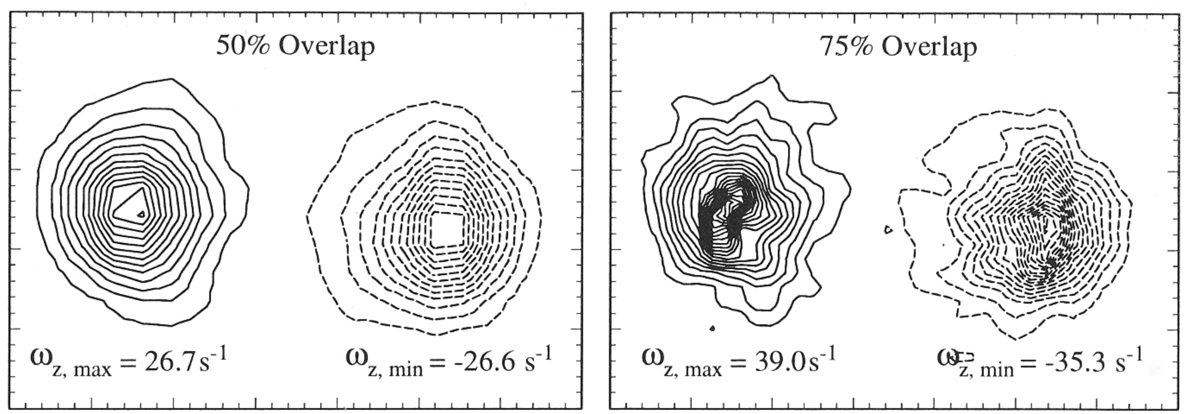

Fig. 6.10. Vorticity field estimates obtained from PIV velocity fields by the circulation method: (left) the velocity field is twice oversampled, (right) four times oversampled. The contours of this laminar vortex pair are known to be smooth such that the nonuniformities are due to measurement noise

❑ Vorticity distribution Examples

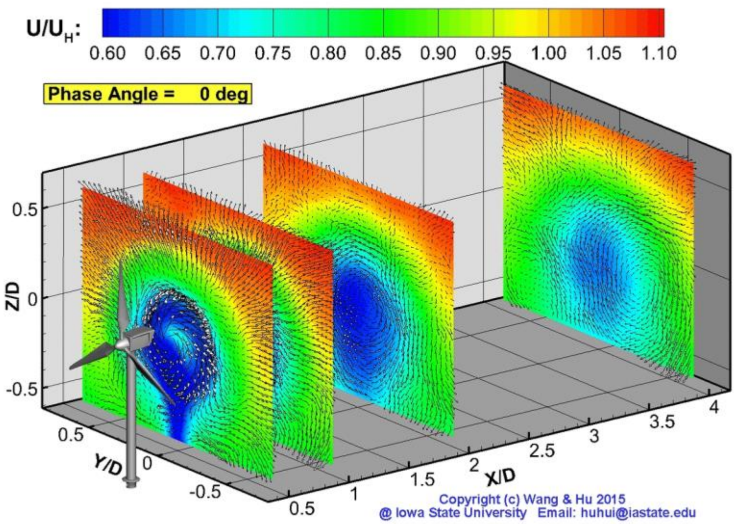

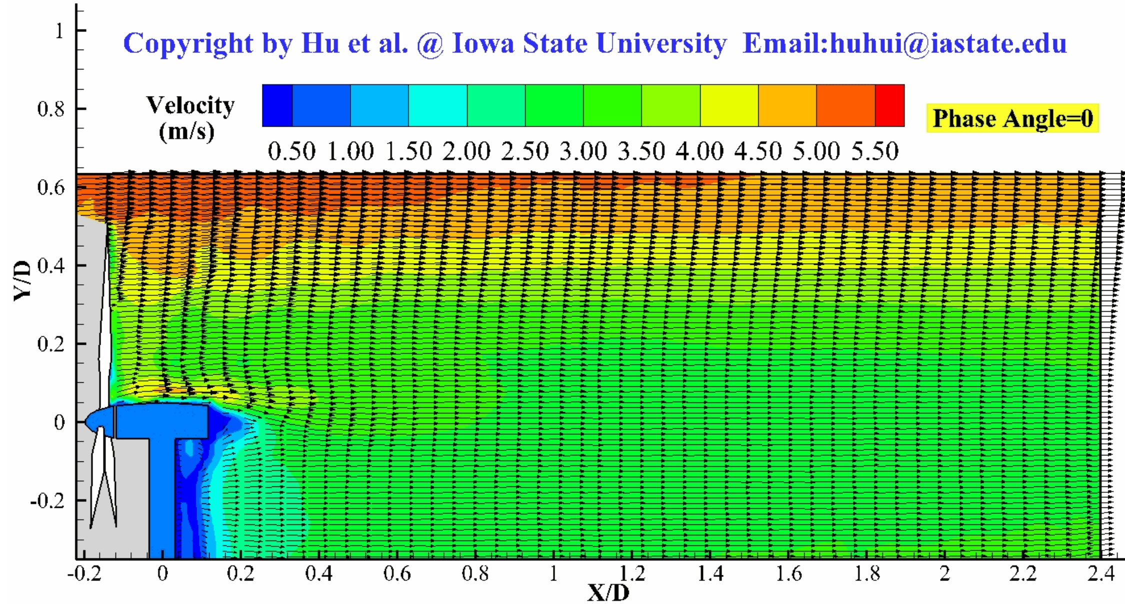

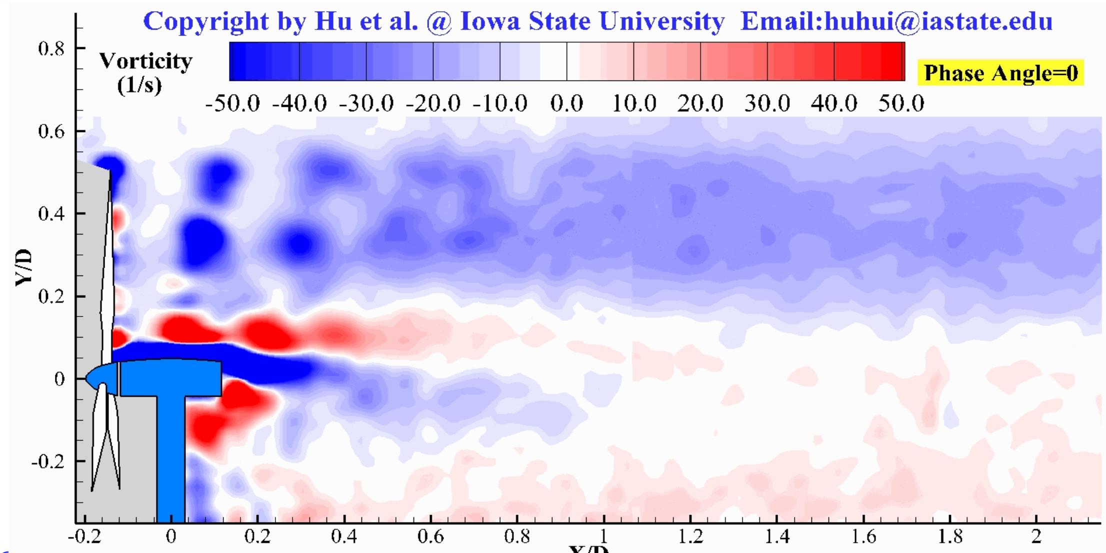

❑ Ensemble-averaged flow quantities

- *Mean velocity components in x, y directions:*

$$U = \sum_{i=1}^{N} u_i / N \qquad V = \sum_{i=1}^{N} v_i / N$$

- *Turbulent velocity fluctuations:*

$$\overline{u'} = \sqrt{\sum_{i=1}^{N} (u_i - U)^2 / N} \qquad \overline{v'} = \sqrt{\sum_{i=1}^{N} (v_i - V)^2}$$

- *Turbulent Kinetic energy distribution:*

$$TKE = \frac{1}{2}\rho(\overline{u'}^2 + \overline{v'}^2)$$

- *Reynolds stress distribution:*

$$\tau = -\rho\overline{u'v'} = -\rho\sum_{i=1}^{N} \frac{(u_i - U)(v_i - U)}{N}$$

❑ Ensemble-averaged Flow Quantities

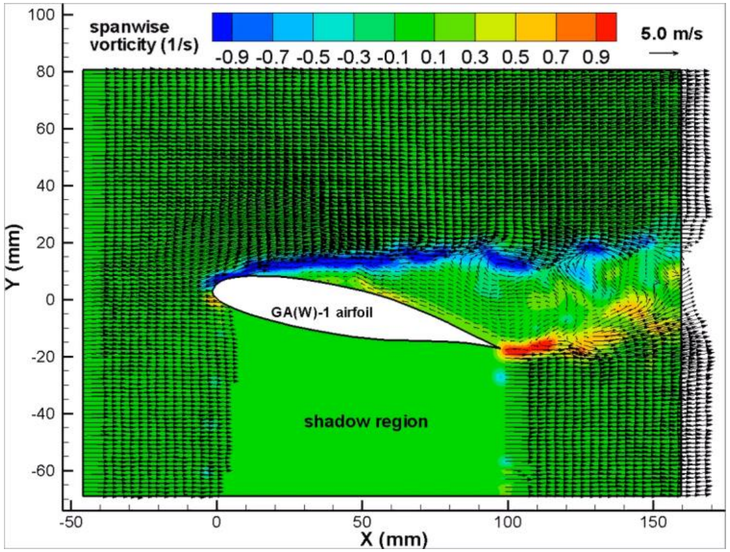

- *Instantaneous PIV result*

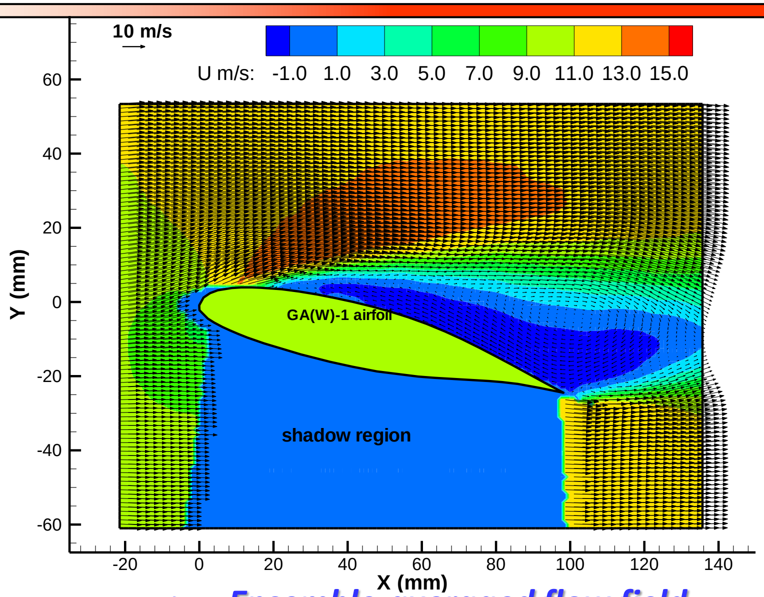

- *Ensemble-averaged flow field*

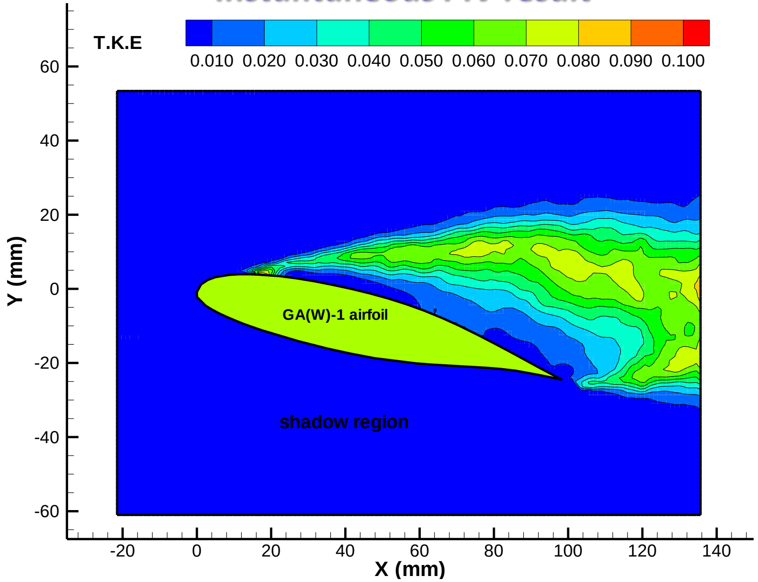

- *Turbulent kinetic energy distribution*

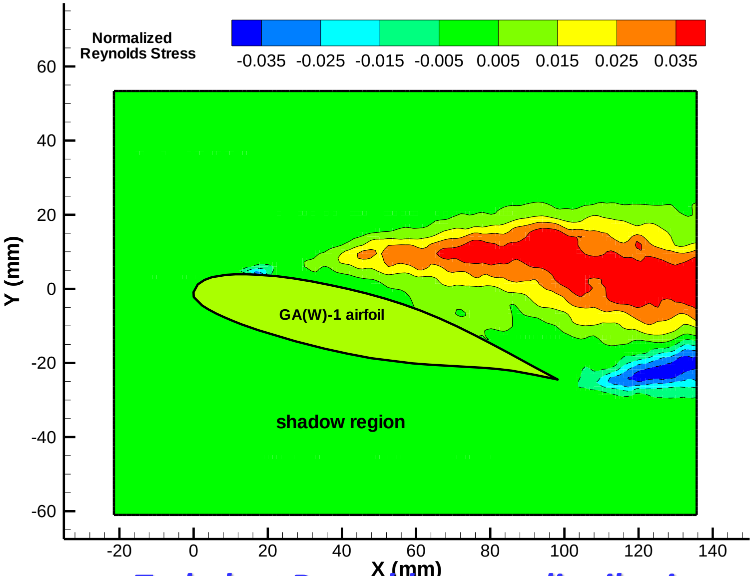

- *Turbulent Reynolds stress distribution*

❑ PRESSURE FIELD ESTIMATION

$$u\frac{\partial u}{\partial x}+v\frac{\partial u}{\partial y}=-\frac{1}{\rho}\frac{\partial p}{\partial x}+\frac{\mu}{\rho}\left(\frac{\partial^2 u}{\partial x^2}+\frac{\partial^2 u}{\partial y^2}\right)$$

$$u\frac{\partial v}{\partial x}+v\frac{\partial v}{\partial y}=-\frac{1}{\rho}\frac{\partial p}{\partial y}+\frac{\mu}{\rho}\left(\frac{\partial^2 v}{\partial x^2}+\frac{\partial^2 v}{\partial y^2}\right)$$

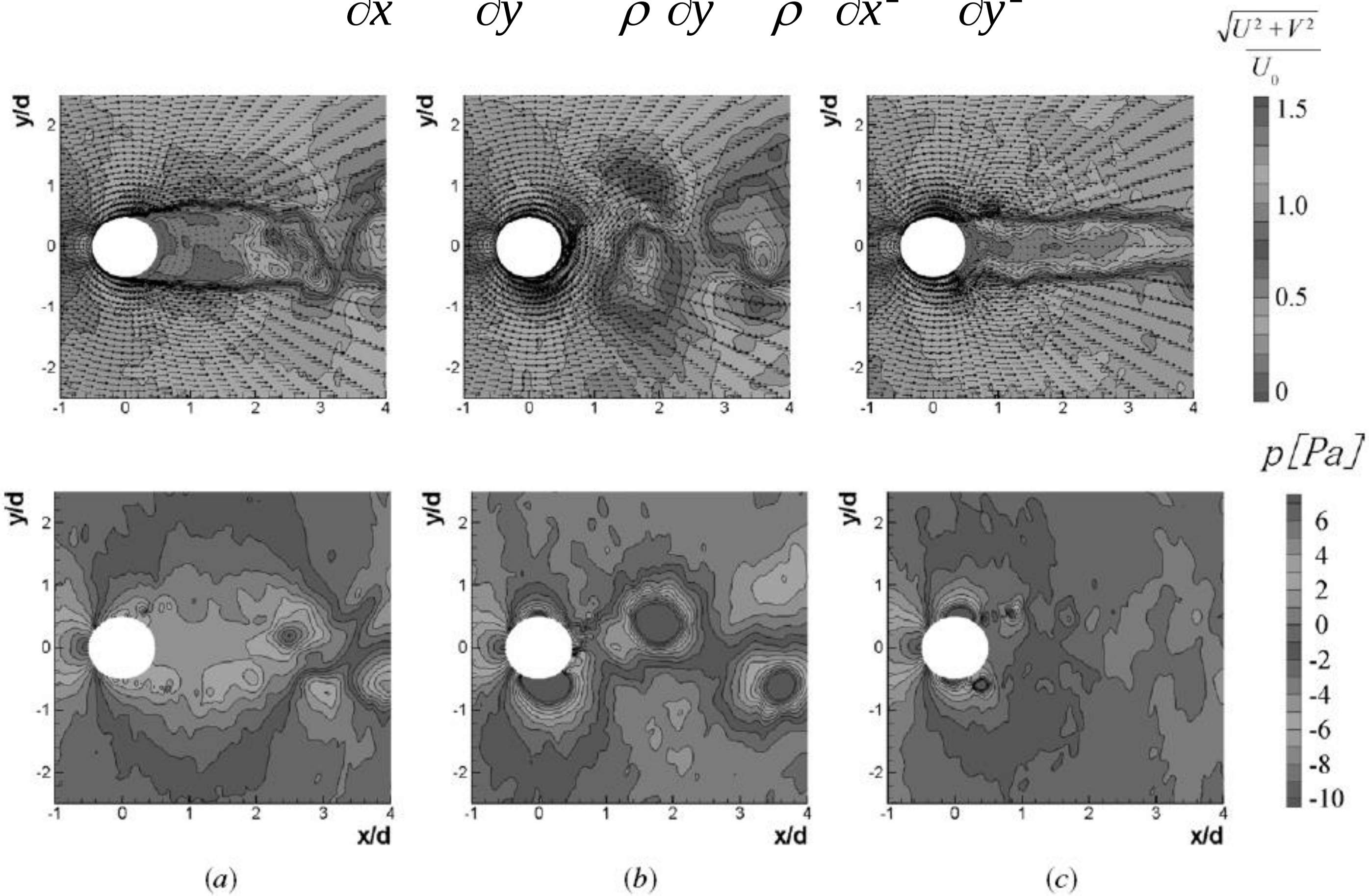

Figure 6. Instantaneous pressure field around a circular cylinder. (*a*) Stationary cylinder, (*b*) low-frequency oscillation ($S_f = 0.2$, $V_r = 2$) and (*c*) high-frequency oscillation ($S_f = 1$, $V_r = 2$).

Integral Force estimation

$$\frac{\partial}{\partial t}\int_{C.V.}\rho\vec{V}\,d\forall+\int_{C.S.}(\rho\vec{V}\vec{V})\bullet d\vec{A}=\int_{C.S.}\tilde{P}\bullet d\vec{A}+\int_{C.V.}\rho\,\vec{f}\,d\forall+\vec{F}$$

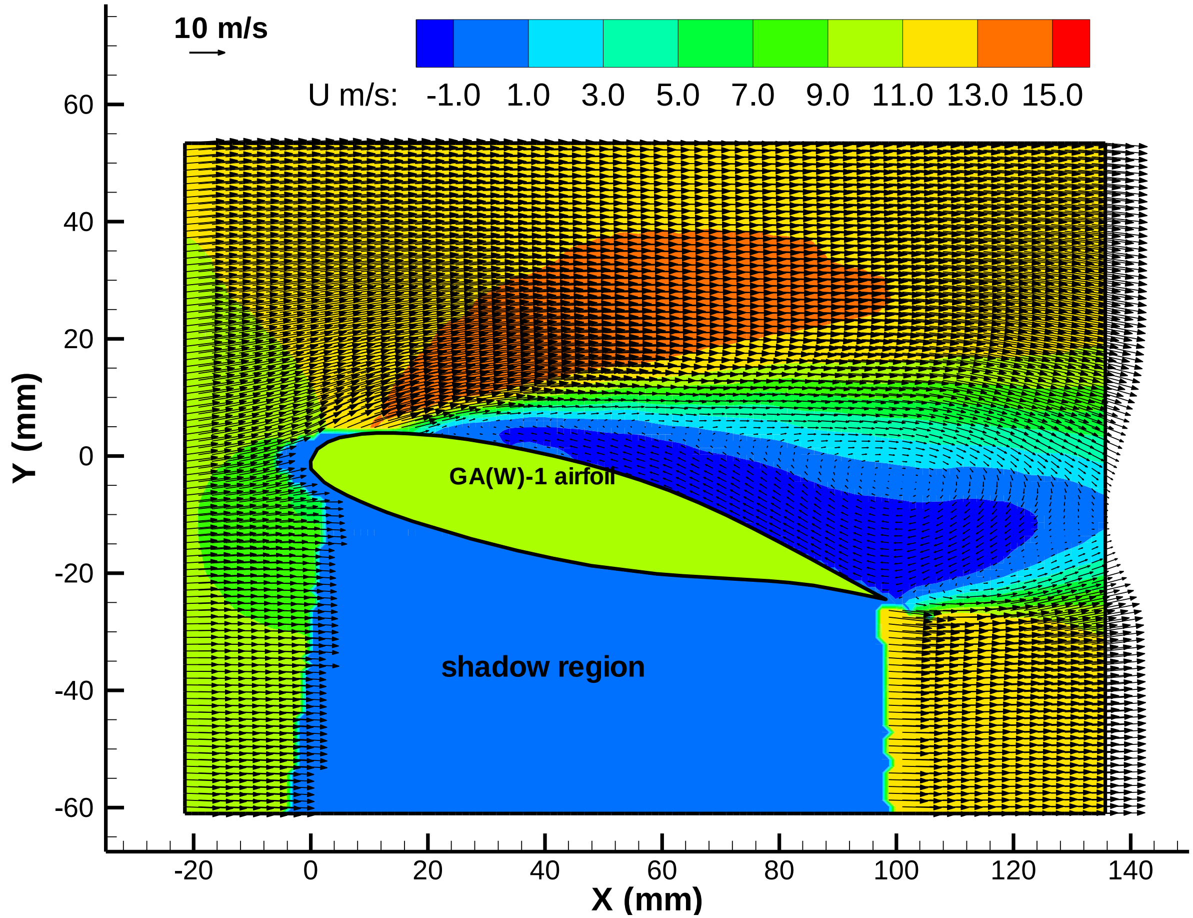

❑ PIV EXAMPLES

- *A supportive COVID-19 study: Experimental Investigation on a Human Sneeze*

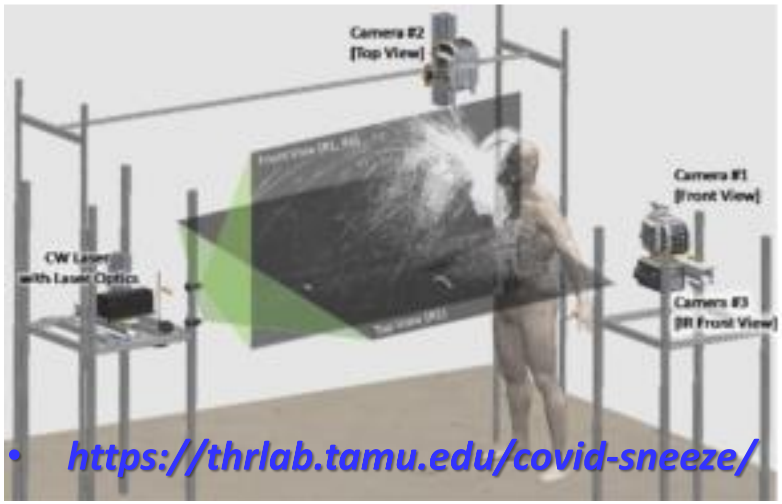

- *https://thrlab.tamu.edu/covid-sneeze/*

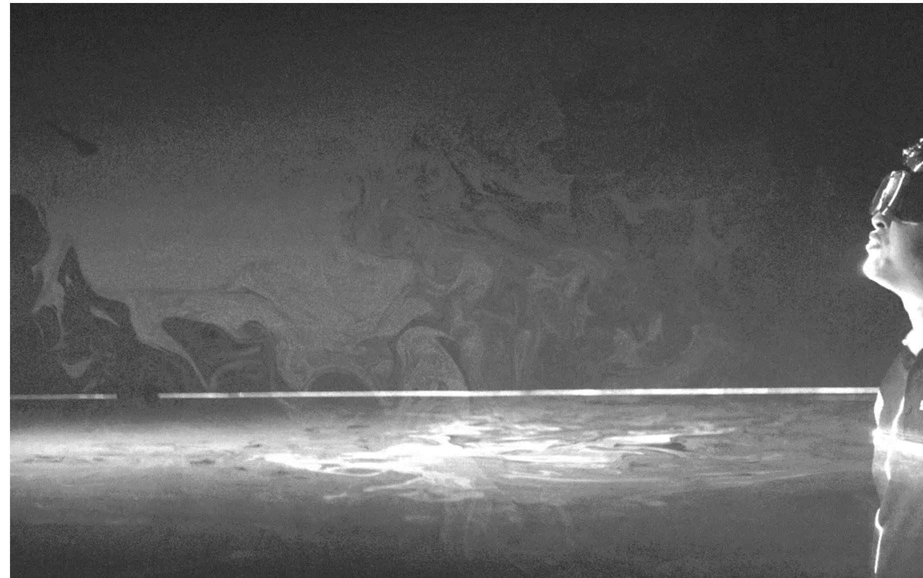

- *https://www.youtube.com/watch?v=9-ui6uFhUx0*